

Inertial measurement with trapped particles: A microdynamical system

E. Rehmi Post,^{a)} George A. Popescu, and Neil Gershenfeld

Center for Bits and Atoms, Massachusetts Institute of Technology, 20 Ames Street, Cambridge, Massachusetts 02139, USA

(Received 4 September 2009; accepted 8 December 2009; published online 5 April 2010)

We describe an inertial measurement device based on an electrodynamically trapped proof mass. Mechanical constraints are replaced by guiding fields, permitting the trap stiffness to be tuned dynamically. Optical readout of the proof mass motion provides a measurement of acceleration and rotation, resulting in an integrated six degree of freedom inertial measurement device. We demonstrate such a device—constructed without microfabrication—with sensitivity comparable to that of commercial microelectromechanical systems technology and show how trapping parameters may be adjusted to increase dynamic range. © 2010 American Institute of Physics. [doi:10.1063/1.3360808]

While micromachined accelerometers and gyroscopes have been commercialized and are approaching the fundamental limits^{1,2} of their noise performance, an inertial measurement unit with six degrees of freedom still requires multiple distinct devices whose dynamic response is limited by their static structure and whose production requires complex microfabrication. Instead of using micromechanical systems we propose here the use of a microdynamical system based on the orbital motion of a trapped particle. This system has no static structure that would require microfabrication (see Fig. 2) yet its microscopic dynamics provide sensitivity and noise performance comparable to that of microelectromechanical systems (MEMS) devices, and its sensitivity and bandwidth can be dynamically controlled.

Our approach follows from the observation that a particle in a Paul trap³ is in effect a spring-mass system with an electrodynamic restoring force. The trap has a hyperbolic electric potential $\Phi(r, t) = \Phi_0(t)\phi(r)(\alpha x^2 + \beta y^2 + \gamma z^2)/a_0^2$ driven by an oscillating voltage $\Phi_0(t) = U + V \cos \Omega t$ and scaled by a geometric factor $a_0^2 = |\alpha|x_0^2 + |\beta|y_0^2 + |\gamma|z_0^2$ defined in terms of the trap's characteristic radii (x_0 , y_0 , and z_0). Absence of free charge in the trap ($\nabla^2\Phi=0$) leads to the constraint $\alpha + \beta + \gamma = 0$. In the case of the three-dimensional (3D) Paul trap, these values are chosen to be $\alpha=1$, $\beta=1$, $\gamma=-2$.

It is well-known that a particle subject to the time-varying electric potential of such a trap experiences fast, small-scale micromotion on the time scale $\tau = 2\pi/\Omega$. Because the electric field in the trap is spatially inhomogeneous, a particle moving in the field will also experience a small net force over one cycle of micromotion. This force leads to the slower, large-scale secular motion of trapped particles.

To derive the effect of inertial acceleration upon a trapped particle, we use the electric pseudopotential of,⁴ defined as,

$$\psi(x) \equiv \frac{eV^2}{2m\Omega^2 a_0^4} x^2. \quad (1)$$

In one dimension, the Hamiltonian for a particle subject to a pseudopotential ψ and an acceleration a is

$$H = \frac{p^2}{2m} + e\psi(x) + mxa = \frac{1}{2m}(p^2 + \kappa x^2) + mxa, \quad (2)$$

where $\kappa = (eV/\Omega a_0^2)^2$. The corresponding equation of motion will be that of a driven harmonic oscillator $\ddot{x} + \omega_s^2 x = -a$ where $\omega_s^2 = \kappa/m$. Substitution of the general solution $x = \bar{x} + c_0 \exp(i\omega_s t) + c_1 \exp(-i\omega_s t)$ shows that the particle oscillates about a mean position

$$\bar{x} = \langle x \rangle = -\frac{1}{\omega_s^2} a = -\frac{m^2 \Omega^2 a_0^4}{e^2 V^2} a. \quad (3)$$

Therefore we see that in the region where the pseudopotential approximation holds, the mean position \bar{x} depends linearly on a .

This analysis was tested by simulating the motion of a charged particle in the trap's electric potential $\Phi(r, t)$. The simulated particle was a gold microsphere of radius $r = 3.125 \mu\text{m}$ and mass $m = 3.85 \text{ ng}$, with trap parameters $U = 0 \text{ V}$, $V = 1000 \text{ V}$, $\Omega = 2\pi \times 240 \text{ rad/s}$, and $a_0 = 0.5 \text{ mm}$. Finally, a Stokes drag term with $b = 6\pi\eta r$ was added to simulate the damping effect of a buffer gas (air at 1 atm with dynamic viscosity $\eta = 1.827 \times 10^{-5} \text{ Pa s}$) resulting in the equations of motion

$$\begin{bmatrix} \ddot{x} \\ \ddot{y} \\ \ddot{z} \end{bmatrix} = \begin{bmatrix} a_x \\ a_y \\ a_z \end{bmatrix} - \frac{6\pi\eta r}{m} \begin{bmatrix} \dot{x} \\ \dot{y} \\ \dot{z} \end{bmatrix} - \frac{2e\Phi}{a_0^2 m} \begin{bmatrix} \alpha x \\ \beta y \\ \gamma z \end{bmatrix}. \quad (4)$$

The results of numerically integrating these equations is shown in Fig. 1, from which it is apparent that the center and amplitude of particle micromotion are both linearly dependent on applied acceleration.

To test these observations experimentally, a planar trap geometry⁵ was chosen for simplicity. Figure 2 shows such a trap with a ring electrode ($x_0 = y_0 = 1.0 \text{ mm}$, $z_0 = 1.3 \text{ mm}$, $\epsilon_r \approx 4.3$) constructed using a circular copper electrode on FR4 circuit board stock. A high-voltage lead drives the central electrode while the brass disk of the transducer and the upper electrode (here, a gold-plated nut) provide the trap's ground references.

The trap is loaded by exciting a piezoelectric transducer with a voltage pulse when the trap electrode is at an appropriate phase to induce charge on the top of a cluster of par-

^{a)}Electronic mail: rehmi.post@cba.mit.edu.

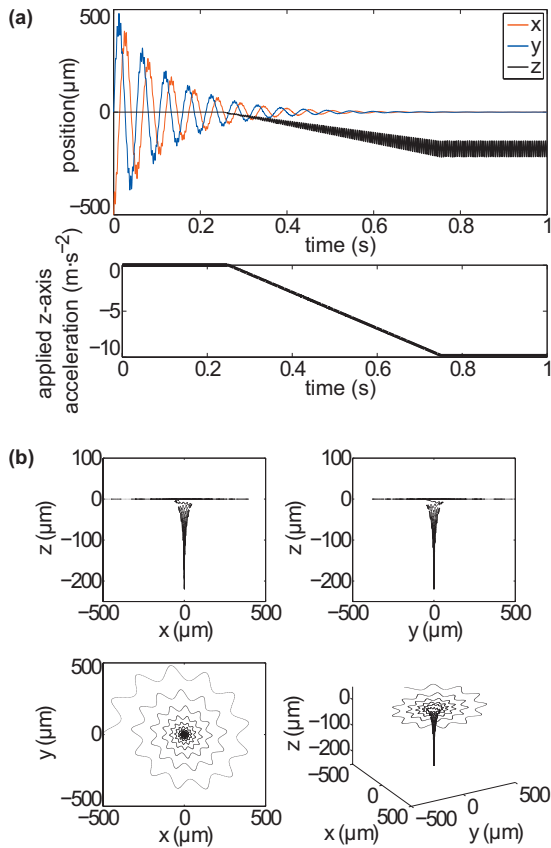


FIG. 1. (Color) Simulation results for a particle launched into the xy plane of a trap in free fall (from $t=0$ s to $t=0.25$ s) and then subject to a linearly increasing downward acceleration (along z) from 0 to 1 g (from $t=0.25$ s to $t=1.0$ s). Data are plotted as (a) position of the particle and applied acceleration over time and (b) projections of particle motion. Simulation parameters are as described in the text. Note that the mean particle displacement \bar{x} is proportional to a .

ticles at ground potential. The ejected particles will carry away an induced charge when they lose contact with ground. Particle charge can be selected by stability of the particle in the trap and calibrated by dynamics of the trap. In these

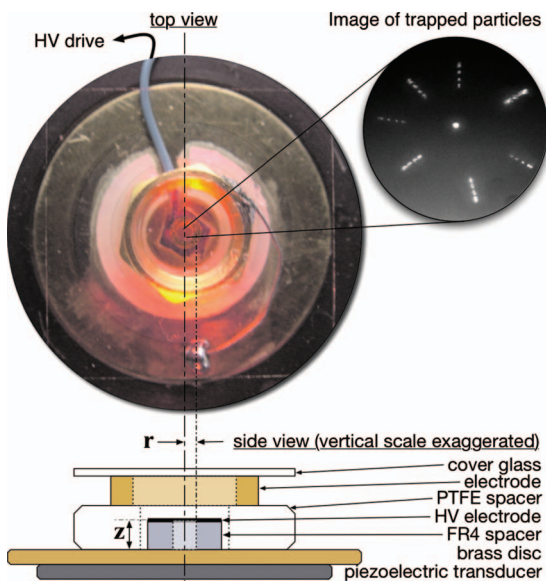


FIG. 2. (Color) Trap construction detail. Dimensions referenced in the figure are $r \approx 500 \mu\text{m}$, $z = 1585 \mu\text{m}$.

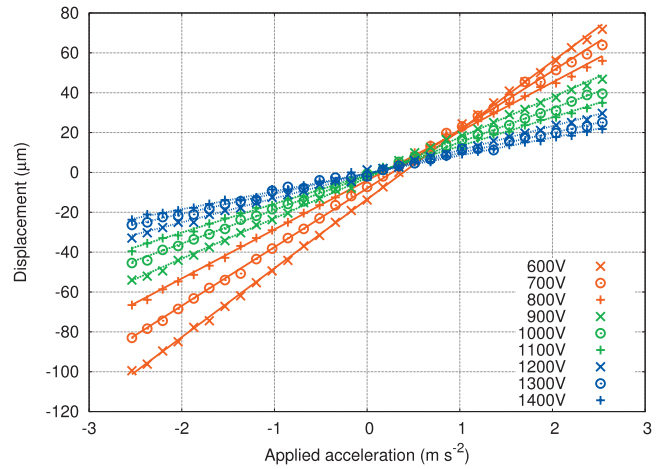


FIG. 3. (Color) Observed particle displacement as a function of applied acceleration (with linear fits).

experiments the particles were gold (Au) microspheres $7.25 \pm 1.5 \mu\text{m}$ in diameter.

A key feature of the inertial measurement trap is its dynamic tunability. Figure 3 shows the displacement of the proof mass as a function of applied acceleration as V varies. Dissipation is introduced to increase stability of the trapped particle's motion⁶ by operating at atmospheric pressure. The pseudopotential must be corrected for drag due to motion in a buffer gas⁷ and the effective spring constant is reduced by damping to $k_{eff} = (e^2 V^2) / 8ma_0^4(\Omega^2 + (b/m)^2)$. Figure 4 shows the measured dependence of k on the AC trap voltage V in our trap, demonstrating its tunability.

The measured effective spring constant can be used to calibrate a measurement of the noise in the trap. When this is done, the observed spectrum shows two distinct regions. Figure 5 plots the observed power spectral density of a measurement of particle drift, with a $1/f$ slope overlaid at low frequencies and a $1/f^2$ slope (diffusion noise⁸) at higher frequencies.

The magnitude of the variance of the measured acceleration can be estimated from the equipartition theorem. For any collection of quadratic energy storage modes in thermal equilibrium each mode will have an average energy equal to $k_B T / 2$ where k_B is Boltzmann's constant (1.38×10^{-23} J/K) and T is the temperature. Energy will be stored

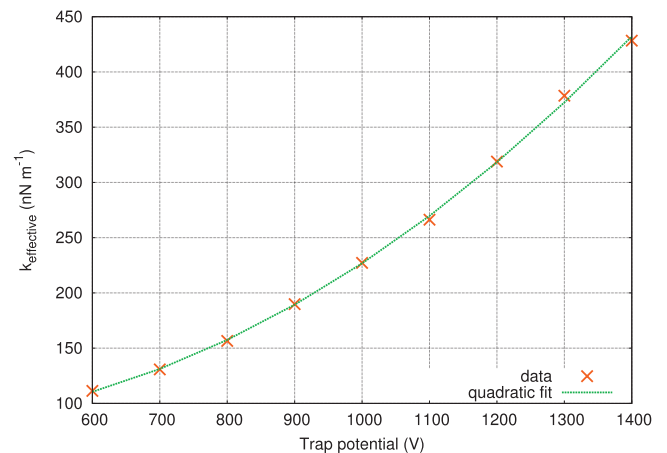


FIG. 4. (Color) Measured effective spring constant as a function of trap voltage.

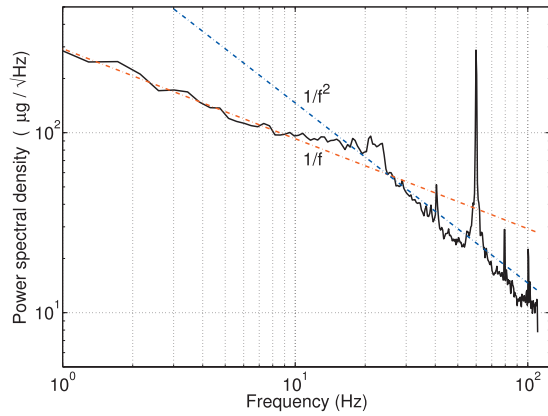


FIG. 5. (Color) Power spectral density of observed particle drift with simulated $1/f$ and diffusion noise spectra overlaid. As the particle passes repeatedly through the Gaussian waist of a focused weak laser beam, its time-domain optical scattering signal reveals the amount of time spent in the beam waist and allows measurement of the particle's closest approach to the optical axis (calibrated by applying known accelerations.) The large peak is from 60 Hz noise, and the side peaks are associated with resonances of the secular motion in the trap potential (verified by simulating the trap dynamics with stochastic forcing).

by a particle's displacement from equilibrium in the pseudopotential ($U=kx^2/2$), so $\langle(\delta x)^2\rangle=k_B T/k$. The scale of thermal noise in acceleration measurements is estimated to be $\langle\delta a\rangle=k\langle\delta x\rangle/m=\sqrt{k k_B T}/m$. Given the observed value of $k=227$ nN/m at $V=1000$ V, the positional variation is expected to be $\langle\delta x\rangle=135$ nm so the rms acceleration noise should be on the order of $\langle\delta a\rangle=812$ μg . This is in good agreement with the integral of the observed noise density which gives an rms noise measurement of 684 μg and is comparable to the performance of state-of-the-art MEMS devices.⁹ From this estimate we can also calculate that trap-

ping effectively cools the proof mass to a temperature $T=213$ K.

The simplicity of microdynamical systems (in this case, the only moving parts are the particles) may lead to devices capable of large dynamic range obtained through closed-loop control of trap stiffness. Such inertial sensors could be simpler to build than their MEMS counterparts yet exhibit superior performance, owing to their dynamically adjustable operating parameters. We propose that similar microdynamical systems could be used as 3D probes for sensing magnetic field strength, fluid flow, and other physical quantities at lower cost and higher performance than comparable MEMS devices.

The authors would like to thank Joe Jacobson, Scott Manalis, and Joe Paradiso for valuable discussions. This work was supported primarily by the MIT Center for Bits and Atoms and NSF under Grant No. CCR-0122419.

¹E. B. Cooper, E. R. Post, S. Griffith, J. Levitan, S. R. Manalis, M. A. Schmidt, and C. F. Quate, *Appl. Phys. Lett.* **76**, 3316 (2000).

²T. B. Gabrielson, *IEEE Trans. Electron Devices* **40**, 903 (1993).

³W. Paul, *Rev. Mod. Phys.* **62**, 531 (1990).

⁴H. G. Dehmelt, *Advances in Atomic and Molecular Physics*, edited by Bates and Estermann (Academic, New York, 1967), Vol. 3, pp. 53–72.

⁵R. G. Brewer, R. G. DeVoe, and R. Kallenbach, *Phys. Rev. A* **46**, R6781 (1992).

⁶V. I. Arnold, V. V. Kozlov, and A. I. Neishtadt, *Mathematical Aspects of Classical and Celestial Mechanics*, 2nd ed. (Springer, Berlin, 1997).

⁷S. Arnold, J. H. Li, S. Holler, A. Korn, and A. F. Izmailov, *J. Appl. Phys.* **78**, 3566 (1995).

⁸D. T. Gillespie, *Am. J. Phys.* **64**, 225 (1996).

⁹The data sheet for the Analog Devices ADXL103 ± 1.7 g single-axis MEMS accelerometer specifies an acceleration noise density of $a_n=110$ $\mu\text{g}/\sqrt{\text{Hz}}$ and a typical rms noise level of $a_n\sqrt{1.6\times\Delta f}=1846$ μg for the bandwidth ($\Delta f=110$ Hz) over which our device was characterized.